

---

# Controllable Image Generation With Composed Parallel Token Prediction

---

**Jamie Stirling**

Department of Computer Science  
Durham University  
Durham, DH1 3LE

jamie.s.stirling@durham.ac.uk

**Noura Al-Moubayed**

Department of Computer Science  
Durham University  
Durham, DH1 3LE

noura.al-moubayed@durham.ac.uk

## Abstract

Compositional image generation requires models to generalise well in situations where two or more input concepts do not necessarily appear together in training (compositional generalisation). Despite recent progress in compositional image generation via composing continuous sampling processes such as diffusion and energy-based models, composing discrete generative processes has remained an open challenge, with the promise of providing improvements in efficiency, interpretability and simplicity. To this end, we propose a formulation for controllable conditional generation of images via composing the log-probability outputs of discrete generative models of the latent space. We first derive a formulation for composing discrete generation processes, enabling generation with an arbitrary number of input conditions without the need for any specialised training loss. We next show how this result can be adapted specifically for parallel token prediction (masked generative transformers) for conditional image generation. Our approach, when applied alongside VQ-VAE and VQ-GAN, achieves state-of-the-art generation accuracy in three distinct settings (FFHQ, Positional CLEVR and Relational CLEVR) while attaining competitive Fréchet Inception Distance (FID) scores. Our method attains an average generation accuracy of 80.71% across the studied settings, representing an average 18.5 percentage-point improvement over the previous state-of-the-art. Our method also outperforms the next-best approach (ranked by accuracy) in terms of FID in seven out of nine experiments, with an average FID of 24.23 (an average improvement of  $-9.58$ ). Furthermore, our method offers a  $2.3\times$  to  $12\times$  speedup over comparable continuous compositional methods on our hardware. We find that our method can generalise to combinations of input conditions that lie outside the training data (e.g. more objects per image) in addition to offering an interpretable dimension of controllability via concept weighting. We further demonstrate that our approach can be readily applied to an open pre-trained discrete text-to-image model without any fine-tuning, allowing for fine-grained control of text-to-image generation. The successful implementation of our framework across diverse compositional settings reinforces its theoretical foundations, while opening up practical avenues for future work in controllable and composable image generation.

## 1 Introduction

Compositional generalisation in deep learning is the capacity of a trained model to respond correctly to *unfamiliar combinations* of *familiar concepts* [1]. The ability of deep learning models to perform compositional generalisation is considered to be a pre-requisite for human-like artificial general intelligence [2], since compositional generalisation is something humans do remarkably well with

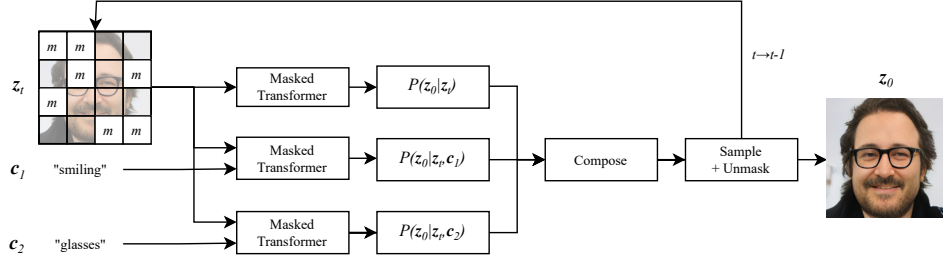


Figure 1: Overview of our approach. At each generation step, *unconditional* and *conditional* unmasking probabilities are obtained, conditioned on the unmasked state and input attributes. Next, our discrete compositional framework is applied, before sampling from the resulting distribution and unmasking a random selection of tokens. This is repeated until a fully unmasked representation of an image is obtained, which is finally decoded into an image.

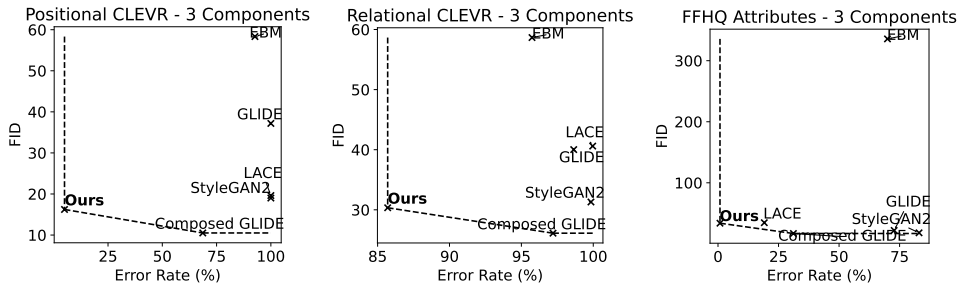


Figure 2: Scatter plots of compositional generation error vs FID on 3 datasets (3 input components): Our method lies on the Pareto front of all results (see Appendix D for full scatter plots) while achieving lowest or joint lowest error among the baselines.

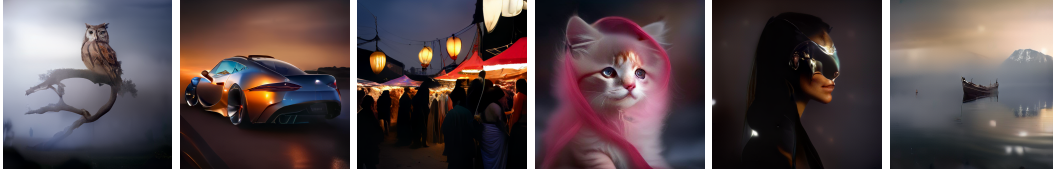
relatively few training examples [3]. Successful compositional generalisation remains an interesting challenge in conditional image generation [4], which involves sampling from very high-dimensional spaces and is the focus of this work.

In the space of diffusion-based and energy-based image generation approaches, earlier works [5, 6, 7] have proposed methods for improving controllability of image generation via *composition* of energy-based and diffusion models. This family of methods enables *conjunction* and *negation* of input concepts by composing the probabilistic outputs of several inference runs with different inputs. While composed techniques exceed non-composed baselines in terms of accuracy and image quality [7], such approaches do not extend to image generation models with *discrete* sample spaces, which offer a number of trade-offs and outright improvements over their continuous counterparts.

Discrete image generation methods include autoregressive sampling approaches [8], and more recently parallel token prediction [9] (also referred to as “absorbing diffusion” and “masked generative transformers” [10, 11]). These methods have been proposed as discrete alternatives to continuous image generation methods (EBM [12] and continuous diffusion [13]). Discrete methods for image generation are necessarily coupled to some method of mapping between high-dimensional pixel space and the discrete latent space, most commonly using VQ-VAE [14] and VQ-GAN [8].

Parallel token methods in particular [9] have a number of advantages over their continuous analogues, including: (1) enabling a direct and controllable trade-off between image quality and sampling speed, (2) offering a second trade-off between accuracy and diversity via a temperature parameter, and (3) allowing in-painting and out-painting without any additional modifications [9, 11]. Until now there has been no way of performing logical *conjunction* and *negation* of concepts on discrete generation pipelines, as is presently possible with diffusion and energy-based models [6, 7].

In this work we derive and evaluate a robust composable image generation approach that combines the advantages of composable generation with those of discrete generative processes. We achieve this by deriving specific formulae to represent logical operations (*conjunction* and *negation* operations) on the probabilistic outputs of discrete generative models. This offers principled and fine-grained



"Ancient oak tree with wide trunk and expansive canopy" AND "Sleek, futuristic finish" AND "Car racing along winding coastal highway at sunset" AND "Owl perched on branch" AND "Vibrant, bustling outdoor market with colorful stalls and shoppers from various cultures" AND "Fluffy kitten with big eyes and pink nose" AND "Woman's face in jeweled masquerade mask covering upper half of face" AND "Rustic, wooden boat floating on misty lake" AND "Soft lighting filtering through mountains in the distance, reflected in mist, golden glow"

Figure 3: Compositional text-to-image results with captions (zooming recommended). Our framework allows the composition of multiple prompts, for fine-grained control of outputs and minimal extra memory requirements.

control of generated outputs. Unlike earlier work in compositional generation, ours is the first (to our knowledge) to apply this idea to a *discrete* generative process [8, 9, 14], i.e. ones which sample from a categorical distribution over a discrete latent space. We provide a fuller and deeper discussion of related work in Appendix A.

We demonstrate empirically that our method of composing discrete generative models can be readily applied to parallel token prediction [9, 11], finding that compositional generalisation accuracy **matches or exceeds the state-of-the-art in 9 out of 9** quantitative experiments across three datasets, representing an average improvement of 18.5 percentage points, while obtaining FID scores that exceed the previous state-of-the-art (ranked by accuracy) in 7 out of 9 quantitative experiments. While each of the three datasets studied represents a distinct and challenging compositional task, our results are obtained using the same hyper-parameters and architecture for all experiments. In addition to the state-of-the-art accuracy and competitive FID scores, sampling images using our approach takes only a fraction of the time of comparable continuous methods on our hardware (Section 3). The relative simplicity of our approach makes it generally applicable to other types of discrete generative model (see Appendix E.2), while also facilitating implementation and integration with existing pre-trained generative models.

Our method further allows the *weighting* of different input conditions (increasing, decreasing or negating the relative importance of each condition in the desired output). This offers an additional layer of controllability over the generated outputs, which we demonstrate in our qualitative experiments. We show that our method can be used with an open pre-trained text-to-image parallel token model (aMUSEd [15]) with satisfying visual results. The successful application of our method to an out-of-the-box and open source pre-trained model broadens the potential for the use of our approach in practical controllable image generation applications. We discuss the broader societal impact of our work in Section 4. The effective implementation of our framework across diverse conditional image generation scenarios offers empirical validation for the mathematical underpinnings of our contribution, meanwhile paving the way for prospective practical applications in the space of controllable conditional image generation.

## 2 Method

In this section we present a method for composing generative models for controllable sampling from discrete representation spaces of images. We first derive a novel formulation that directly informs our method of composing conditional distributions over discrete spaces. Next we show how this extends generally to all discrete sequential generation tasks, in which categorical variables are sampled iteratively to produce a complete sample (e.g. via autoregressive or masked models). We show how this result can be specifically adapted for conditional parallel token prediction [9, 11] to achieve high-quality and accurate controllable image synthesis. This is further enhanced by concept weighting, which allows the relative importance of input conditions to be modified to the desired effect. We note that similar results can be obtained for other generative priors (provided they are

iterative and discrete, see Appendix E.2 for example). This section lays the groundwork for our later experiments with compositional sampling from the latent space of VQ-VAE and VQ-GAN.

## 2.1 Composing conditional categorical distributions

Our framework is derived from the simplifying assumption that the input conditions  $c_1, \dots, c_n$  are statistically independent of each other. A consequence of this is that probability of an outcome  $x$  given two or more conditions  $c_1, c_2, \dots$  is proportional to the product of the probabilities of each condition given  $x$ . Intuitively, taking the product of different categorical distributions in this way is analogous to taking the intersection of the sample spaces of two or more conditional distributions, thus (in the ideal scenario) resulting in samples which embody all of the specified conditions [16]. We discuss the benefits and limitations of this assumption in Section 4. Following previous work with composition of continuous models [2, 7], we factorize the distribution of a  $k$ -way categorical variable  $x$  conditioned on  $n$  variables as follows:

$$P(x|c_1, \dots, c_n) \propto P(x) \prod_{i=1}^n P(c_i|x) \quad (1)$$

Applying Bayes' theorem [17], this can be re-written as:

$$\begin{aligned} P(x|c_1, \dots, c_n) &\propto P(x) \prod_{i=1}^n \frac{P(x|c_i)P(c_i)}{P(x)} \\ &\propto P(x) \prod_{i=1}^n \frac{P(x|c_i)}{P(x)} \end{aligned} \quad (2)$$

We are able to eliminate the  $P(c_i)$  term in (2) as a consequence of normalising the values of  $P(x = x_i|\dots)$  for all  $x_i$  such that they sum to 1 (see Appendix E.1 for full derivation).

## 2.2 Composition for sequential generative tasks

So far we have shown how our approach applies to conditional generation with a single categorical output  $x$ . In practice, many generative tasks involve sampling multiple categorical variables (tokens or latent codes) over a number of time steps [18, 19] where the sampling of a new state  $s_{t+1}$  at each successive step  $t$  is conditioned on the previous state (in addition to the specified conditions  $c_1, \dots, c_n$ ). Formulating this alongside the result in (2) gives the following general expression for composing discrete sequential generation tasks:

$$P(s_{t+1}|s_t, c_1, \dots, c_n) \propto P(s_{t+1}|s_t) \prod_{i=1}^n \frac{P(s_{t+1}|s_t, c_i)}{P(s_{t+1}|s_t)} \quad (3)$$

We observe that this applies generally to any generative process in which each successive step is conditioned on the output of previous steps, including autoregressive language modelling [19], masked language modelling [20], as well as autoregressive [8] and non-autoregressive [9] approaches for image generation. In the remainder of this paper, we maintain a particular focus on conditional parallel token prediction, which we use for composed sampling from the latent space of VQ-VAE [14] and VQ-GAN [8] for high-fidelity image synthesis.

A key practical consideration concerning the result in (3) is that estimates must be obtained for each conditional probability distribution  $P(s_{t+1}|s_t, c_i)$  in addition to  $P(s_{t+1}|s_t)$ . In each of our experiments (Section 3) we ensure that, during training, conditional information is zero-masked with a set probability (0.1) per sample, thus allowing us to obtain  $P(s_{t+1}|s_t)$  at inference time by supplying zeros instead of the condition encoding.

## 2.3 Composed parallel token prediction

Parallel token prediction [9, 10, 11] is a non-autoregressive alternative to next-token prediction [8] for generative sampling from a discrete latent space. This allows a direct trade-off between sampling speed and image generation quality [9] by controlling the rate at which tokens are sampled. Parallel

token prediction can be thought of as the gradual un-masking of a collection of discrete latent codes  $\mathbf{z}_0$  given the partial reconstruction from a previous time step (as well as additional conditioning information). This corresponds directly to the next-state prediction formulation in (3), but with the time labels  $t$  reversed in order to reflect the “reverse process” which characterizes diffusion models (both continuous [21] and discrete [9]):

$$P(\mathbf{z}_{t-1}|\mathbf{z}_t, \mathbf{c}_1, \dots, \mathbf{c}_n) \propto P(\mathbf{z}_{t-1}|\mathbf{z}_t) \prod_{i=1}^n \frac{P(\mathbf{z}_{t-1}|\mathbf{z}_t, \mathbf{c}_i)}{P(\mathbf{z}_{t-1}|\mathbf{z}_t)} \quad (4)$$

In (4),  $\mathbf{z}_t$  is an intermediate, partially unmasked representation at each time step, and  $\mathbf{z}_{t-1}$  represents the distribution over image representations with fewer masked tokens. In practise, following earlier work with parallel token prediction, the model is trained to directly predict the fully unmasked representation  $\mathbf{z}_0$  (as opposed to intermediate states) so as to maximise training stability [9]. At inference time, we compute the composed unmasking probabilities as:

$$P(\mathbf{z}_0|\mathbf{z}_t, \mathbf{c}_1, \dots, \mathbf{c}_n) \propto P(\mathbf{z}_0|\mathbf{z}_t) \prod_{i=1}^n \frac{P(\mathbf{z}_0|\mathbf{z}_t, \mathbf{c}_i)}{P(\mathbf{z}_0|\mathbf{z}_t)} \quad (5)$$

Where each  $P(\dots)$  term corresponds to a feed-forward operation which takes a partially unmasked state as input, optionally with additional conditioning information  $\mathbf{c}_i$ . Image representations can then be unmasked one or more tokens at a time, corresponding to a trade-off between sample speed (more tokens per iteration) and image generation quality (fewer tokens per iteration) [9].

## 2.4 Concept weighting for improved controllability

Following earlier work with composable diffusion models for image generation [7], we introduce an additional set of hyperparameters  $w_1, \dots, w_n$  which correspond to the relative weight to be assigned to each condition  $\mathbf{c}_1, \dots, \mathbf{c}_n$  respectively. Restating (3) in terms of log-probabilities and introducing these weighting terms gives:

$$\log P(\mathbf{s}_{t+1}|\mathbf{s}_t, \mathbf{c}_1, \dots, \mathbf{c}_n) = \log P(\mathbf{s}_{t+1}|\mathbf{s}_t) + \sum_{i=1}^n w_i [\log P(\mathbf{s}_{t+1}|\mathbf{s}_t, \mathbf{c}_i) - \log P(\mathbf{s}_{t+1}|\mathbf{s}_t)] \quad (6)$$

This expression (6) can straightforwardly be manipulated into the appropriate form for parallel token prediction (4). A key observation here is that setting a concept weight  $w_i$  to *negative* (e.g.  $-1$ ) has the intuitive effect of *negating* the corresponding condition  $\mathbf{c}_i$  by excluding image representations which correspond to  $\mathbf{c}_i$  from the sample space. Altogether, the prompt-weighting approach provides an additional degree of controllability over model outputs by enabling conditions to be emphasized ( $w_i > 1$ ), de-emphasized ( $w_i < 1$ ) or even negated ( $w_i < 0$ ) as desired. We demonstrate the practical utility of this feature in our qualitative experiments (Section 3).

In practice, we use our compositional framework to sample from the discrete latent space of VQ-VAE [14] and VQ-GAN [8], which are powerful and practical approaches for encoding images and other high-dimensional modalities as collections of discrete latent codes (visual tokens) while maintaining high-fidelity reconstructions and generated samples.

## 2.5 Discrete encoding and decoding of images

In order to compose categorical distributions for generating images, we must also define an invertible mapping between RGB images and discrete latent representations. We utilise a convolutional down-sampling and up-sampling (autoencoder) to map between RGB image space and latent embedding space. Following the original VQ-VAE [14] formulation, we employ nearest-neighbour vector quantization, in which encoder outputs are mapped to their nearest neighbour in a learned codebook. Specifically, for each encoder output vector  $z_e$ , the corresponding quantized vector is computed as the nearest codebook entry  $e_c$ , where:

$$c = \arg \min_j \|z_e - e_j\|_2 \quad (7)$$

where  $e_0, e_1 \dots e_{K-1}$  are entries in a learned vector codebook of length  $K$ .

Since the quantization step is non-differentiable, it is necessary to estimate the gradients during backpropagation. For this purpose, straight-through gradient estimation [22] is used, whereby during backpropagation the gradients are copied directly from the decoder input  $z_c$  to the encoder output  $z_e$ . We use this vector quantization approach for all our experiments, which includes the embedding and commitment loss terms from the original VQ-VAE formulation [14].

### 3 Experiments

#### 3.1 Datasets

Following earlier work [7] in evaluating compositional generalisation for image generation, we employ three datasets for training and evaluation: Positional CLEVR [7, 23], Relational CLEVR [7, 23] and FFHQ [24] (full description of datasets in Appendix B). These three datasets are chosen to represent a range of unique and challenging compositional tasks. For each of the three datasets, we train a VQ-VAE or VQ-GAN model to enable encoding and decoding between the image space and the discrete latent representation space, in addition to a conditional parallel token prediction model (encoder-only transformer) which learns to unmask discrete latent representations, optionally conditioned on an (encoded) input annotation. We compare our results on these datasets to results from 6 baselines reported by [7].

#### 3.2 Model training

We train a VQ-GAN model to reconstruct FFHQ samples at  $256 \times 256$  resolution, as well as VQ-VAE models for each of CLEVR and Relational CLEVR at  $128 \times 128$  resolution. These choices of resolution follow earlier work in compositional generation with these 3 datasets [7]. We find in practice that VQ-VAE (without the adversarial loss) is sufficient for high-fidelity reconstruction of the two CLEVR datasets due to the smaller resolution and visual simplicity, while VQ-GAN is required for realistic reconstructions of FFHQ. Unlike [7], our choice of training regime produces FFHQ images directly at  $256 \times 256$ , so a post-upsampling step is not required during evaluation. We train with a perceptual loss [25] in addition to the MSE loss for all datasets (and the learned adversarial loss for FFHQ). Full details of model training are in Appendix G.

#### 3.3 Quantitative evaluation of compositional generation

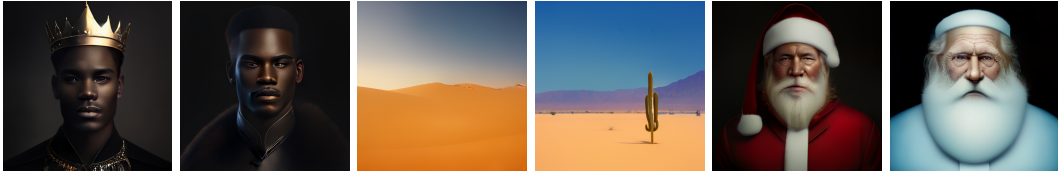
For each dataset, following [7] we evaluate (compositionally) generated image samples according to both image quality (FID [26]) and binary classification accuracy (corresponding to whether a specified attribute, or collection of attributes, is present in the corresponding generated output image). We repeat all such experiments for 1, 2 and 3 attributes per image for all 3 datasets, totalling 9 quantitative experiments. We use a temperature of 0.9 when generating samples for our quantitative experiments. Details of how accuracy scores are obtained are in Appendix I.

In comparison to 6 baseline results (including the previous state-of-the-art [7]) our approach is state-of-the-art for accuracy, **outperforming or matching the accuracy of the previous state-of-the-art**, while attaining highly competitive FID (Fréchet Inception Distance [26]) scores across the three datasets. Particularly noteworthy are our accuracy results for Positional CLEVR, for which our method scores 99.30%, 98.18% and 95.04% on 1, 2 and 3 input components respectively, where the previous state-of-the-art scored 86.42%, 59.20% and 31.36% respectively (Table 1). We see similarly dramatic improvements much harder Relational CLEVR dataset (Appendix Table 3) and significant improvements on the FFHQ dataset (Appendix Table 4).

We speculate that the dramatic accuracy improvements offered by our method can be attributed to the fact that the introduction of the discrete representation learning step (VQ-VAE or VQ-GAN) facilitates the learning of an expressive and compositional “visual language” to represent images, while the conditional parallel token model offers a strongly regularised and highly calibrated model for the visual language. We conjecture that these effects compound to produce an efficient, accurate and robust compositional method.

Table 1: Quantitative results (accuracy and FID score) on the Positional CLEVR dataset

Method	1 Component		2 Components		3 Components	
	Acc (%) $\uparrow$	FID $\downarrow$	Acc (%) $\uparrow$	FID $\downarrow$	Acc (%) $\uparrow$	FID $\downarrow$
StyleGAN2-ADA [27]	37.28 $\pm$ 1.37	57.41	-	-	-	-
StyleGAN2 [28]	1.04 $\pm$ 0.29	51.37	0.04 $\pm$ 0.04	23.29	0.00 $\pm$ 0.00	19.01
LACE [5]	0.70 $\pm$ 0.24	50.92	0.00 $\pm$ 0.00	22.83	0.00 $\pm$ 0.00	19.62
GLIDE [29]	0.86 $\pm$ 0.26	61.68	0.06 $\pm$ 0.06	38.26	0.00 $\pm$ 0.00	37.18
EBM [6]	70.54 $\pm$ 1.29	78.63	28.22 $\pm$ 1.27	65.45	7.34 $\pm$ 0.74	58.33
Composed GLIDE [7]	<u>86.42<math>\pm</math>0.97</u>	<u>29.29</u>	<u>59.20<math>\pm</math>1.39</u>	<u>15.94</u>	<u>31.36<math>\pm</math>1.31</u>	<b>10.51</b>
Ours	<b>99.30<math>\pm</math>0.24</b>	<b>13.76</b>	<b>98.18<math>\pm</math>0.38</b>	<b>15.30</b>	<b>95.04<math>\pm</math>0.61</b>	<u>16.23</u>



[\*] "a king **not** wearing a crown, portrait" AND [\*] "a sunny desert "a sunny desert, land- [\*] "santa claus **not** "santa claus, portrait" a crown, portrait" (NOT "wearing a with no sand dunes, scape" AND (NOT wearing red, portrait" AND (NOT "wearing red") crown") landscape" "sand dunes")

Figure 4: Concept negation with text-to-image: Our method allows more precise control over the outputs of an existing pre-trained model (aMUSEd [15]). Images are in pairs with the baseline result on the left and our method on the right.

### 3.4 Qualitative experiments

In addition to the quantitative evaluation of our method against the baselines, here we also qualitatively investigate the usefulness of our approach outside of rigorous experimental settings. In particular, we investigate the controllability offered by logical conjunction and negation of prompts, as well as the qualitative effect of concept weighting. In addition to the 3 models trained for our quantitative experiments, some of the experiments below apply our method to a pre-trained text-to-image model that uses parallel token prediction ([11]). We choose the aMUSEd [15] implementation of MUSE because it is open and publicly accessible (as of the time of writing), in addition to being trained on a large, open-source dataset [30], which facilitates the open-ended generation which we aim to explore here. Additional qualitative results are in the Appendix.

**Concept negation:** Fig. 4 demonstrates the application of the negation (**NOT**) operator using aMUSEd text-to-image parallel token prediction [15]. We compare each example against a single-prompt baseline using the same model. We focus on problematic cases where the underlying text-image model is incapable of properly interpreting negation in the linguistic sense, which is especially pertinent when the concept being negated is widely considered an essential characteristic of the concept from which it is being negated (e.g. “a king **not** wearing a crown”). Our method allows us to achieve more specific outputs without changing or fine-tuning the underlying model, even in cases where the underlying model fails to comprehend the original negated prompt.

**Out-of-distribution generation:** Here we demonstrate our model’s ability to generalise to compositions of conditions that are not seen in training. We focus on the (positional) CLEVR dataset, in which individual training samples have at most 5 objects per image. Fig.5 contains generated samples for input conditions specifying between 6 and 8 objects per image. We make two key observations of Fig.5: (1) that our method successfully generalises outside the distribution of the training data and (2) that re-running the same input gives varied outputs (the model has not over-fit to always generate the same objects in the same position).

**Varying the concept weight:** Fig.6 illustrates the effect of varying the concept weighting parameter  $w$  for a specific input condition (in this case, the weighting of the “male” attribute of FFHQ). Keeping other concept weights the same ( $w_{smile} = 3.0$ ,  $w_{no\_glasses} = 3.0$ ), we vary  $w_{male}$  from  $-3.0$  to  $3.0$ , finding that typically “male” traits are embodied most strongly in the outputs where  $w_{male} > 0$ , and typically “female” traits are embodied most strongly in outputs where  $w_{male} < 0$ . In addition, the

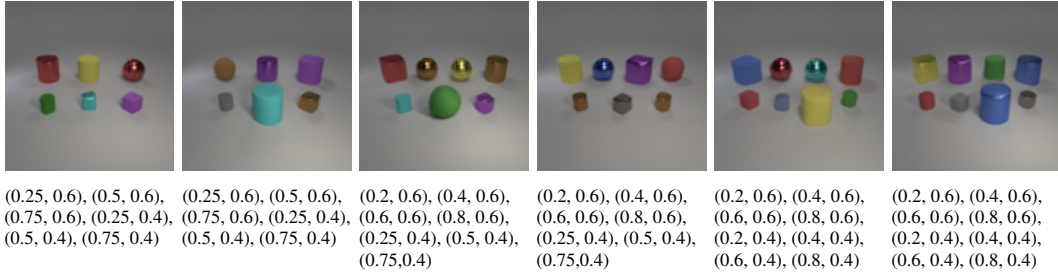


Figure 5: Compositional out-of-distribution generation: Positional CLEVR training images contain no more than 5 objects per image, but our compositional method allows 6 or more objects to appear in the same image via compositional sampling.

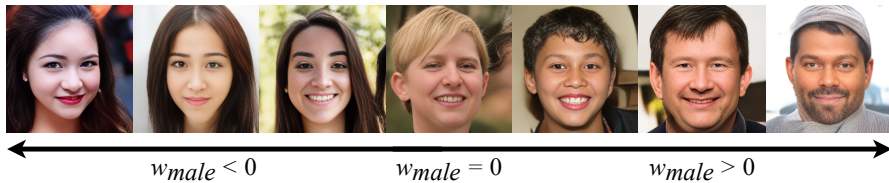


Figure 6: Effect of varying concept weight  $w_{male}$  for our model trained on the FFHQ dataset: Concept weighting (both positive and negative) allows for fine-grained control of output attributes.

expression of gender-typical visual traits appear to increment as  $w_{male}$  goes from positive to negative (notably, with the appearance of facial hair as  $w_{male} \rightarrow 3.0$  and red lipstick as  $w_{male} \rightarrow -3.0$ ). This is consistent with the expectation that the concept weighting capability of our method should allow for a continuum of controllability over the generated outputs. Meanwhile, non-controlled visual traits such as hair colour and facial phenotype remain diverse as the  $w_{male}$  parameter is varied. We include similar visualisations for the other two FFHQ attributes in Appendix F.2.

### 3.5 Parameter count and sampling time

Table 2 contains a comparison of our method to the most similar methods in the literature (composed EBM [6] and composed GLIDE [7]). We compare our method against these methods in particular for 2 reasons: (1) they are compositional and iterative like our own method, and (2) they are generally closest to ours (highest) in terms of accuracy on the three datasets studied. We compare in terms of total parameters and the time taken to generate both a single image and a batch of 25 images on our hardware (NVIDIA GeForce RTX 3090) with 3 input conditions (Positional CLEVR dataset). Runs of baseline methods use the official PyTorch implementations from [7] with default settings (corresponding to the baseline results in Tables 1,3 and 4). The results in Table 2 show that our method runs in a fraction of the time of existing approaches while having a comparable number of parameters (and superior accuracy: see Table 1 and Tables 3 and 4 in Appendix C). Altogether, we see a  $2.3\times$  to  $12.0\times$  speedup across our speed experiments compared with the continuous iterative baselines.

## 4 Discussion

Through varied quantitative and qualitative experiments, we have demonstrated that our formulation for compositional generation with iterative sampling methods is readily applicable to a range of tasks for both newly trained and out-of-the-box pre-trained models. We demonstrated state-of-the-art performance in terms of the accuracy of the generated results, in addition to obtaining competitive sample quality as measured by FID scores. This is achieved with minimal extra cost in terms of memory, since only the log-probability outputs need to be cached at inference time. The simplicity of our approach in comparison to existing compositional methods offers further advantages, including ease of implementation (facilitating integration with existing discrete generation pipelines) in addition to improved interpretability, since the composition operator can be thought of as directly taking the intersection between two discrete distributions.



Table 2: Parameter counts and sample times for 3 input components (ours vs. baselines)

Method	Total parameters (millions)	Sample time / img (s)	Sample time / batch of 25 (s)
EBM	33	5.99±0.17	108.57±0.93
Composed GLIDE	385	4.92±0.17	73.92±0.70
Ours	108	<b>2.11±0.39</b>	<b>9.08±0.39</b>

The strong quantitative metrics of our method are complemented by its *out-of-distribution* generation capability and *controllability*. The significance of the results of our quantitative experiments is further reinforced by the fact that we used the same experimental settings for all three of the datasets studied, without extensive fine-tuning of hyperparameters, training runs or model architecture. Our method further provides a  $2.3\times$  to  $12\times$  speedup over comparable approaches on our hardware.

#### 4.1 Limitations

Similarly to compositional methods for continuous processes [7], our method requires  $n + 1$  times the number of feed-forward operations compared to standard iterative approaches of the same architecture, where  $n$  is the number of conditions imposed on the output. This is a direct consequence of the mathematical formulation of the approach, however this is largely mitigated by the fact that our method can produce accurate and high-quality outputs in only a small number of iterations [6, 7].

Our method makes a strong assumption that input conditions are independent ( $P(c_1, c_2) = P(c_1)P(c_2)$  for all conditions  $c_1, c_2$ ). It is possible in practical scenarios that this underlying assumption of our approach is in some way violated, for example due to biases in the training data. The importance-weighting capability of our method can mitigate this in part by allowing the user to compensate for potential biases, however we speculate that greater robustness would be better achieved through an unbiased backbone model. Training unbiased models for image generation is beyond the scope of this work and remains an open challenge, especially in the context of text-to-image generation [31]. Further to this, we have not yet explored specialised methods for choosing the condition weighting coefficients  $w_i$ , which may be an interesting direction for future work (e.g. producing a learned concept-weighting policy).

#### 4.2 Broader impacts

We have shown that our method can be applied directly to a publicly available pre-trained discrete text-to-image model without any fine-tuning to achieve fine-grained control over visual generation. While this presents an opportunity for positive impact by enabling creative works, we also wish to raise attention to the broader impact of our work from the perspectives of both *societal bias* and *misuse*. Image generation techniques in particular can be susceptible to perpetuating or even amplifying societal biases [32], and our method will inherit whatever biases are present in the training data or pre-trained model. In addition, readily accessible and controllable image generation presents opportunities for *misuse*, for example for the purposes of misinformation [33] as well as defamation and impersonation [34].

## 5 Conclusion

We have proposed a novel method for enabling precisely controllable conditional image generation by composing discrete iterative generative process. Our method can be combined with VQ-VAE and VQ-GAN to achieve state-of-the-art compositional generation accuracy and across 3 diverse datasets while maintaining competitive FID scores. We further show that our approach can be applied an out-of-the-box pre-trained text-to-image model to allow for controllable generation. Meanwhile, sampling speed is faster than comparable methods using the same hardware and a comparable number of parameters. Though far outside the scope of our present work with controllable image generation, the prospect of applying our method for other compositional tasks (such as multi-prompt text generation) remains an intriguing possibility for future work. Altogether, we believe our work lays a strong foundation for future work in the direction of controllable generation via composed parallel token prediction.

## References

- [1] Baihan Lin, Djallel Bouneffouf, and Irina Rish. A survey on compositional generalization in applications. *arXiv preprint arXiv:2302.01067*, 2023.
- [2] Zhenlin Xu, Marc Niethammer, and Colin A Raffel. Compositional generalization in unsupervised compositional representation learning: A study on disentanglement and emergent language. *Advances in Neural Information Processing Systems*, 35:25074–25087, 2022.
- [3] Ronald Boris Dekker, Fabian Otto, and Christopher Summerfield. Determinants of human compositional generalization. 2022.
- [4] Kaiyi Huang, Kaiyue Sun, Enze Xie, Zhenguo Li, and Xihui Liu. T2i-compbench: A comprehensive benchmark for open-world compositional text-to-image generation. In A. Oh, T. Neumann, A. Globerson, K. Saenko, M. Hardt, and S. Levine, editors, *Advances in Neural Information Processing Systems*, volume 36, pages 78723–78747. Curran Associates, Inc., 2023.
- [5] Weili Nie, Arash Vahdat, and Anima Anandkumar. Controllable and compositional generation with latent-space energy-based models. *Advances in Neural Information Processing Systems*, 34:13497–13510, 2021.
- [6] Yilun Du, Shuang Li, and Igor Mordatch. Compositional visual generation with energy based models. *Advances in Neural Information Processing Systems*, 33:6637–6647, 2020.
- [7] Nan Liu, Shuang Li, Yilun Du, Antonio Torralba, and Joshua B Tenenbaum. Compositional visual generation with composable diffusion models. In *Computer Vision–ECCV 2022: 17th European Conference, Tel Aviv, Israel, October 23–27, 2022, Proceedings, Part XVII*, pages 423–439. Springer, 2022.
- [8] Patrick Esser, Robin Rombach, and Björn Ommer. Taming transformers for high-resolution image synthesis, 2020.
- [9] Sam Bond-Taylor, Peter Hesse, Hiroshi Sasaki, Toby P. Breckon, and Chris G. Willcocks. Unleashing transformers: Parallel token prediction with discrete absorbing diffusion for fast high-resolution image generation from vector-quantized codes. In *European Conference on Computer Vision (ECCV)*, 2022.
- [10] Huiwen Chang, Han Zhang, Lu Jiang, Ce Liu, and William T Freeman. Maskgit: Masked generative image transformer. In *Proceedings of the IEEE/CVF Conference on Computer Vision and Pattern Recognition*, pages 11315–11325, 2022.
- [11] Huiwen Chang, Han Zhang, Jarred Barber, AJ Maschinot, Jose Lezama, Lu Jiang, Ming-Hsuan Yang, Kevin Murphy, William T Freeman, Michael Rubinstein, et al. Muse: Text-to-image generation via masked generative transformers. *arXiv preprint arXiv:2301.00704*, 2023.
- [12] Yilun Du and Igor Mordatch. Implicit generation and modeling with energy based models. *Advances in Neural Information Processing Systems*, 32, 2019.
- [13] Jonathan Ho, Ajay Jain, and Pieter Abbeel. Denoising diffusion probabilistic models. *Advances in neural information processing systems*, 33:6840–6851, 2020.
- [14] Aaron Van Den Oord, Oriol Vinyals, et al. Neural discrete representation learning. *Advances in neural information processing systems*, 30, 2017.
- [15] Suraj Patil, William Berman, Robin Rombach, and Patrick von Platen. amused: An open muse reproduction. *arXiv preprint arXiv:2401.01808*, 2024.
- [16] G.E. Hinton. Products of experts. *9th International Conference on Artificial Neural Networks: ICANN '99*, 1999:1–6, 1999.
- [17] James Joyce. Bayes’ theorem. 2003.

- [18] Tom B. Brown, Benjamin Mann, Nick Ryder, Melanie Subbiah, Jared Kaplan, Prafulla Dhariwal, Arvind Neelakantan, Pranav Shyam, Girish Sastry, Amanda Askell, Sandhini Agarwal, Ariel Herbert-Voss, Gretchen Krueger, Tom Henighan, Rewon Child, Aditya Ramesh, Daniel M. Ziegler, Jeffrey Wu, Clemens Winter, Christopher Hesse, Mark Chen, Eric Sigler, Mateusz Litwin, Scott Gray, Benjamin Chess, Jack Clark, Christopher Berner, Sam McCandlish, Alec Radford, Ilya Sutskever, and Dario Amodei. Language Models are Few-Shot Learners. *Advances in Neural Information Processing Systems*, 2020-December, 5 2020.
- [19] Ashish Vaswani, Noam Shazeer, Niki Parmar, Jakob Uszkoreit, Llion Jones, Aidan N. Gomez, Łukasz Kaiser, and Illia Polosukhin. Attention Is All You Need. *Advances in Neural Information Processing Systems*, 2017-December:5999–6009, 6 2017.
- [20] Jacob Devlin, Ming Wei Chang, Kenton Lee, and Kristina Toutanova. BERT: Pre-training of Deep Bidirectional Transformers for Language Understanding. *NAACL HLT 2019 - 2019 Conference of the North American Chapter of the Association for Computational Linguistics: Human Language Technologies - Proceedings of the Conference*, 1:4171–4186, 10 2018.
- [21] Prafulla Dhariwal and Alexander Nichol. Diffusion models beat gans on image synthesis. *Advances in neural information processing systems*, 34:8780–8794, 2021.
- [22] Yoshua Bengio, Nicholas Léonard, and Aaron Courville. Estimating or propagating gradients through stochastic neurons for conditional computation. *arXiv preprint arXiv:1308.3432*, 2013.
- [23] Justin Johnson, Bharath Hariharan, Laurens Van Der Maaten, Li Fei-Fei, C Lawrence Zitnick, and Ross Girshick. Clevr: A diagnostic dataset for compositional language and elementary visual reasoning. In *Proceedings of the IEEE conference on computer vision and pattern recognition*, pages 2901–2910, 2017.
- [24] Tero Karras, Samuli Laine, and Timo Aila. A style-based generator architecture for generative adversarial networks. In *Proceedings of the IEEE/CVF conference on computer vision and pattern recognition*, pages 4401–4410, 2019.
- [25] Richard Zhang, Phillip Isola, Alexei A Efros, Eli Shechtman, and Oliver Wang. The unreasonable effectiveness of deep features as a perceptual metric. In *Proceedings of the IEEE conference on computer vision and pattern recognition*, pages 586–595, 2018.
- [26] Martin Heusel, Hubert Ramsauer, Thomas Unterthiner, Bernhard Nessler, and Sepp Hochreiter. Gans trained by a two time-scale update rule converge to a local nash equilibrium. *Advances in neural information processing systems*, 30, 2017.
- [27] Tero Karras, Miika Aittala, Janne Hellsten, Samuli Laine, Jaakko Lehtinen, and Timo Aila. Training generative adversarial networks with limited data. *Advances in neural information processing systems*, 33:12104–12114, 2020.
- [28] Tero Karras, Samuli Laine, Miika Aittala, Janne Hellsten, Jaakko Lehtinen, and Timo Aila. Analyzing and improving the image quality of stylegan. In *Proceedings of the IEEE/CVF conference on computer vision and pattern recognition*, pages 8110–8119, 2020.
- [29] Alex Nichol, Prafulla Dhariwal, Aditya Ramesh, Pranav Shyam, Pamela Mishkin, Bob McGrew, Ilya Sutskever, and Mark Chen. Glide: Towards photorealistic image generation and editing with text-guided diffusion models. *arXiv preprint arXiv:2112.10741*, 2021.
- [30] Christoph Schuhmann, Romain Beaumont, Richard Vencu, Cade Gordon, Ross Wightman, Mehdi Cherti, Theo Coombes, Aarush Katta, Clayton Mullis, Mitchell Wortsman, et al. Laion-5b: An open large-scale dataset for training next generation image-text models. *Advances in Neural Information Processing Systems*, 35:25278–25294, 2022.
- [31] Yixin Wan, Arjun Subramonian, Anaelia Ovalle, Zongyu Lin, Ashima Suvarna, Christina Chance, Hritik Bansal, Rebecca Pattichis, and Kai-Wei Chang. Survey of bias in text-to-image generation: Definition, evaluation, and mitigation. *arXiv preprint arXiv:2404.01030*, 2024.
- [32] Alexandra Sasha Luccioni, Christopher Akiki, Margaret Mitchell, and Yacine Jernite. Stable bias: Analyzing societal representations in diffusion models. *arXiv preprint arXiv:2303.11408*, 2023.

- [33] Charlotte Bird, Eddie Ungless, and Atoosa Kasirzadeh. Typology of risks of generative text-to-image models. In *Proceedings of the 2023 AAAI/ACM Conference on AI, Ethics, and Society*, pages 396–410, 2023.
- [34] Yisroel Mirsky and Wenke Lee. The creation and detection of deepfakes: A survey. *ACM computing surveys (CSUR)*, 54(1):1–41, 2021.
- [35] Geoffrey E Hinton. Training products of experts by minimizing contrastive divergence. *Neural computation*, 14(8):1771–1800, 2002.
- [36] Seniha Esen Yuksel, Joseph N Wilson, and Paul D Gader. Twenty years of mixture of experts. *IEEE transactions on neural networks and learning systems*, 23(8):1177–1193, 2012.
- [37] Saeed Masoudnia and Reza Ebrahimpour. Mixture of experts: a literature survey. *Artificial Intelligence Review*, 42:275–293, 2014.
- [38] Michael I Jordan and Robert A Jacobs. Hierarchical mixtures of experts and the em algorithm. *Neural computation*, 6(2):181–214, 1994.
- [39] Xue Bin Peng, Glen Berseth, and Michiel Van de Panne. Terrain-adaptive locomotion skills using deep reinforcement learning. *ACM Transactions on Graphics (TOG)*, 35(4):1–12, 2016.
- [40] Chen Tessler, Shahar Givony, Tom Zahavy, Daniel Mankowitz, and Shie Mannor. A deep hierarchical approach to lifelong learning in minecraft. In *Proceedings of the AAAI conference on artificial intelligence*, volume 31, 2017.
- [41] Carlos Riquelme, Joan Puigcerver, Basil Mustafa, Maxim Neumann, Rodolphe Jenatton, André Susano Pinto, Daniel Keysers, and Neil Houlsby. Scaling vision with sparse mixture of experts. *Advances in Neural Information Processing Systems*, 34:8583–8595, 2021.
- [42] Noam Shazeer, Azalia Mirhoseini, Krzysztof Maziarz, Andy Davis, Quoc Le, Geoffrey Hinton, and Jeff Dean. Outrageously large neural networks: The sparsely-gated mixture-of-experts layer. *arXiv preprint arXiv:1701.06538*, 2017.
- [43] Xue Bin Peng, Michael Chang, Grace Zhang, Pieter Abbeel, and Sergey Levine. Mcp: Learning composable hierarchical control with multiplicative compositional policies. In H. Wallach, H. Larochelle, A. Beygelzimer, F. d'Alché-Buc, E. Fox, and R. Garnett, editors, *Advances in Neural Information Processing Systems*, volume 32. Curran Associates, Inc., 2019.
- [44] Ali Razavi, Aaron Van den Oord, and Oriol Vinyals. Generating diverse high-fidelity images with vq-vae-2. *Advances in neural information processing systems*, 32, 2019.
- [45] Robert Gray. Vector quantization. *IEEE Assp Magazine*, 1(2):4–29, 1984.
- [46] Jacob Devlin, Ming-Wei Chang, Kenton Lee, and Kristina Toutanova. Bert: Pre-training of deep bidirectional transformers for language understanding. *arXiv preprint arXiv:1810.04805*, 2018.

## Appendix

### A Related Work

#### A.1 Product of experts

The concept of compositional generalisation relates intimately to advanced approaches in probabilistic modelling, especially the "product of experts" (PoE) framework. PoE is designed to combine multiple probabilistic models operating on the same input space [35], leveraging each of their strengths to improve generalisation. This approach is particularly powerful in contexts involving high-dimensional data that adhere to multiple constraints [16]. Each "expert" within a PoE framework focuses on a subset of constraints, with the final outputs assigning high probability to outputs that satisfy constraints imposed by all experts. Our work adapts this idea to the compositional generation of images in discrete spaces, and is the first to our knowledge to apply the product-of-experts paradigm to iterative generative processes over multiple successive time-steps.

## A.2 Composition of continuous diffusion models

Earlier works proposed methods for conditioning energy-based [5, 6] and diffusion models [7] respectively based on the conjunction and negation of input attributes, drawing on formal analogues to PoE [16]. [7] introduces an approach that enhances the capabilities of text-conditioned diffusion models in generating complex and photo-realistic images based on textual descriptions. Our method draws inspiration from these ideas (principally in proposing formal derivations of probabilistic conjunction and negation operators), however our mathematical formulation diverges significantly due to the fact that our method applies to *discrete* iterative approaches (compare with EBM and diffusion, which operate in a continuous output space [12, 13]). The novelty of our derivation, and its application to discrete generation go beyond the literature by offering a novel formulation for composing iterative discrete generation models, while empirically achieving state-of-the-art in image generation accuracy while attaining competitive FID scores.

## A.3 Mixture of experts

Mixture-of-experts is a particularly well-studied paradigm in machine learning and deep learning [36, 37], in which the core principle is to combine the outputs of multiple specialised models to improve overall performance on a task, often with some form of gating mechanism [38]. Mixture-of-experts has seen numerous successful applications spanning reinforcement learning [39, 40], vision [41], and large language models [42]. These approaches are characterised by the presence of multiple feed-forward processes that occur in parallel, while the outputs are “switched” between experts [37]. This idea shares some similarities with our work, in which we combine the outputs from multiple feed-forward runs. Two of the major differences in our work are (1) that the “experts” of our approach are actually the same model being used with different input conditions, and (2) that outputs are composed via a *multiplicative* process rather than an additive/gated process (see “Product of experts” above).

## A.4 Composition in sequential tasks

Earlier work in reinforcement learning [43] has sought to use ideas relevant to our own for composing *policies* for the purposes of compositional generalisation in multi-timestep environments. The main idea shared with our work is that of *multiplying* constituent “primitives” (as opposed to *additive* composition, as in mixture-of-experts [37]). According to [43], the benefit of this multiplicative approach over mixture-of-experts is that multiple policies can be expressed in the same sequence. This bears some superficial similarities to our work with compositional discrete image generation, in which multiple attributes are required to be expressed in the same output image, however it differs greatly the application and formalism.

## A.5 Discrete representation learning and Sampling

Discrete representation learning has emerged as the discrete counterpart to continuous VAE approaches [14, 44]. Discrete representation learning is based on the concept of vector-quantization (VQ) [45], whereby features from a continuous vector space are mapped to an element of a finite set of learned codebook vectors. This VQ family of models includes VQ-VAE [14] and VQ-GAN [8]. VQ-family approaches require a secondary prior model to be trained to sample from the discrete latent space, which can be computationally expensive at both train- and inference- time [8, 9, 14].

A more recent sampling approach aims to address this with parallel token prediction using a transformer encoder [9, 11, 15] (akin to masked language modelling [46]), which introduces a controllable trade-off between sample speed and generation quality, as well as the ability to control the diversity of outputs via temperature. The per-image generation time is still linear in the size ( $W \times H$ ) of the image, albeit with a smaller constant than autoregressive models [9]. The advantages of parallel token prediction over autoregressive approaches motivate our work in producing a method for composing discrete image sampling approaches.

VQ-family models form a critical component of our work due to their utility in learning a mapping between high-dimensional RGB images and a more compact discrete latent space, while our contribution offers a new dimension of controllability over previous sampling approaches. This

Table 3: Quantitative results (accuracy and FID score) on the Relational CLEVR dataset

Method	1 Component		2 Components		3 Components	
	Acc (%) $\uparrow$	FID $\downarrow$	Acc (%) $\uparrow$	FID $\downarrow$	Acc (%) $\uparrow$	FID $\downarrow$
StyleGAN2-ADA [27]	67.71 $\pm$ 1.32	20.55	-	-	-	-
StyleGAN2 [28]	20.18 $\pm$ 1.14	22.29	1.66 $\pm$ 0.36	30.58	0.16 $\pm$ 0.11	31.30
LACE [5]	1.10 $\pm$ 0.30	40.54	0.10 $\pm$ 0.09	40.61	0.04 $\pm$ 0.04	40.60
GLIDE [29]	46.20 $\pm$ 1.41	<b>17.61</b>	8.86 $\pm$ 0.80	<b>28.56</b>	1.36 $\pm$ 0.33	40.02
EBM [6]	<b>78.14</b> $\pm$ 1.17	44.41	24.16 $\pm$ 1.21	55.89	4.26 $\pm$ 0.57	58.66
Composed GLIDE [7]	60.40 $\pm$ 1.38	29.06	21.84 $\pm$ 1.17	29.82	2.80 $\pm$ 0.47	<b>26.11</b>
Ours	<b>78.16</b> $\pm$ 1.17	30.00	<b>43.06</b> $\pm$ 1.40	<u>28.87</u>	<b>14.30</b> $\pm$ 0.99	<u>30.34</u>

Table 4: Quantitative results (accuracy and FID score) on the FFHQ dataset

Method	1 Component		2 Components		3 Components	
	Acc (%) $\uparrow$	FID $\downarrow$	Acc (%) $\uparrow$	FID $\downarrow$	Acc (%) $\uparrow$	FID $\downarrow$
StyleGAN2-ADA [27]	91.06 $\pm$ 0.81	<b>10.75</b>	-	-	-	-
StyleGAN2 [28]	58.90 $\pm$ 1.39	18.04	30.68 $\pm$ 1.30	18.06	16.96 $\pm$ 1.06	18.06
LACE [5]	97.60 $\pm$ 0.43	28.21	95.66 $\pm$ 0.58	36.23	80.88 $\pm$ 1.11	34.64
GLIDE [29]	98.66 $\pm$ 0.33	20.30	48.68 $\pm$ 1.41	22.69	27.24 $\pm$ 1.26	21.98
EBM [6]	98.74 $\pm$ 0.32	89.95	93.10 $\pm$ 0.72	99.64	30.01 $\pm$ 1.30	335.70
Composed GLIDE [7]	<u>99.26</u> $\pm$ 0.24	18.72	92.68 $\pm$ 0.74	<b>17.22</b>	68.86 $\pm$ 1.31	<b>16.95</b>
Ours	<b>99.78</b> $\pm$ 0.13	21.52	<b>99.38</b> $\pm$ 0.22	28.25	<b>99.18</b> $\pm$ 0.26	33.80

provides additional benefits such as concept weighting and out-of-distribution generation which we demonstrate in our experiments (Section 3).

## B Full Dataset Details

Below we provide a full description of each dataset used in the quantitative evaluation of our method.

- **FFHQ** [24]: FFHQ is a dataset of 70,000 aligned images of human faces. Three binary attribute labels are available for each image: "smile"/"no smile", "glasses"/"no glasses", "male"/"female", which we use to condition the generation process.
- **Positional CLEVR** [23]: CLEVR is a synthetic dataset of rendered 3D objects of various colours, shapes, sizes and textures. In the Positional variant of CLEVR, object attribute and position annotations are available. Following [7], we use a 30,000-image subset of CLEVR (restricted to contain between 1 and 5 objects per image). For this task, image generation is conditioned on object position only.
- **Relational CLEVR** [7, 23]: Relational CLEVR is similar in appearance to Positional CLEVR, with the addition of text annotations for objects and their relationships (e.g. "*the red cube is above the blue sphere*"). Image generation is conditioned on (tokenized) text descriptions of object attributes and relationships, including object shape, size, material, colour, and relative position.

## C Quantitative Results for Relational CLEVR and FFHQ

Tables 3 and 4 contain the results of our quantitative experiments (Accuracy and FID) for the Relational CLEVR and FFHQ Datasets. These are discussed in the main text but omitted for brevity.

## D Error vs FID Plots

Figures 7, 8 and 9 are scatter plots of error (100%-accuracy) against FID corresponding to results in Tables 1, 3 and 4. Included on the same axes of each plot are the empirical Pareto front of the data, which we define as the unique linear piece-wise form that is convex, monotonic, and is as close as

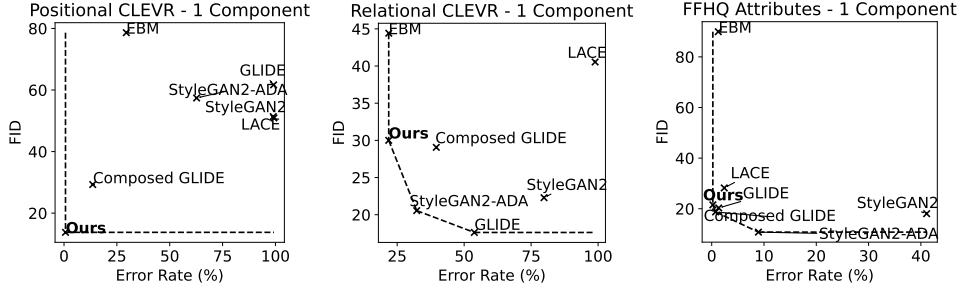


Figure 7: Scatter plots of compositional generation error vs FID on 3 datasets (1 input component): Our method lies on the Pareto front of all results while achieving state-of-the-art (lowest or joint lowest) error.

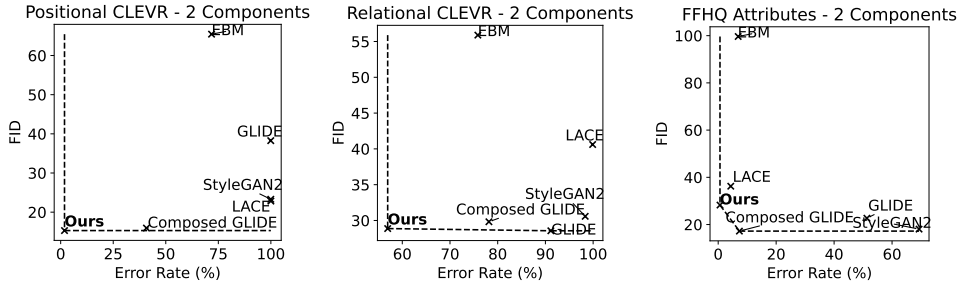


Figure 8: Scatter plots of compositional generation error vs FID on 3 datasets (2 input component): Our method lies on the Pareto front of all results while achieving state-of-the-art (lowest or joint lowest) error.

possible to the lowermost and leftmost (best) of the data points while extending to the top and right of each plot. Our results all lie on, or very close to, the Pareto front of their respective plots while having the lowest error rate when ranked among the baselines.

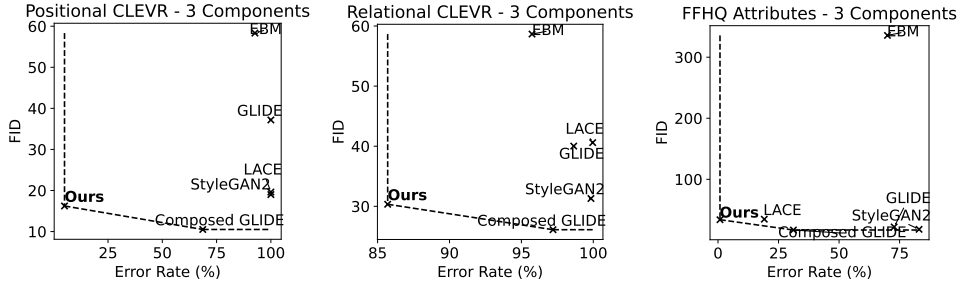


Figure 9: Scatter plots of compositional generation error vs FID on 3 datasets (3 input component): Our method lies on the Pareto front of all results while achieving state-of-the-art (lowest or joint lowest) error.

## E Derivations

Here we include additional derivations which were omitted from the main paper for brevity.

## E.1 Cancelling the $P(c_i)$ terms

The following is a full derivation of the result given in (2) of the main text.

$$P(\mathbf{x} = x_j | \mathbf{c}_1, \dots, \mathbf{c}_n) = \frac{P(\mathbf{x} = x_j) \prod_{i=1}^n \frac{P(\mathbf{x}=x_j|\mathbf{c}_i)P(\mathbf{c}_i)}{P(\mathbf{x}=x_j)}}{\sum_{u=1}^k \left[ P(\mathbf{x} = x_u) \prod_{i=1}^n \frac{P(\mathbf{x}=x_u|\mathbf{c}_i)P(\mathbf{c}_i)}{P(\mathbf{x}=x_j)} \right]} \quad (8)$$

$$= \frac{P(\mathbf{x} = x_j) \prod_{i=1}^n \frac{P(\mathbf{x}=x_j|\mathbf{c}_i)}{P(\mathbf{x}=x_j)}}{\sum_{u=1}^k \left[ P(\mathbf{x} = x_u) \prod_{i=1}^n \frac{P(\mathbf{x}=x_u|\mathbf{c}_i)}{P(\mathbf{x}=x_u)} \right]} \quad (9)$$

In this way, the contribution of  $P(c_i)$  terms is cancelled out, since  $P(c_i)$  are constant with respect to different values of  $x_j$ . In subsequent sections, we show how this brief but important result for conditional categorical distributions can be successfully extended to both next-token and parallel token prediction for images, achieving state-of-the-art accuracy and speed on 3 datasets.

## E.2 Compositional Next-Token Prediction

In the main text we claim that our discrete compositional method can be applied to arbitrary generative methods provided they are discrete and iterative. Here we back up this claim by showing how our method can be adapted to autoregressive (next-token) sampling.

In the specific case of discrete autoregressive image modelling, a single latent code (token) is generated at each time step, conditioned on some initial context in addition to previously generated tokens. In this situation, each successive state  $\mathbf{s}_{t+1}$  is simply the concatenation of the previous state  $\mathbf{s}_t$  and the subsequent generated token  $\mathbf{x}_{t+1}$ . Thus the random variable  $\mathbf{s}_{t+1}$  can be restated as:

$$\mathbf{s}_{t+1} = \mathbf{s}_t \oplus \mathbf{x}_{t+1} \quad (10)$$

where  $\oplus$  denotes the concatenation of two tokens or strings of tokens. Consequently, the conditional generation task in (3) can be reformulated in terms of sampling the next token given the previous state:

$$P(\mathbf{x}_{t+1} | \mathbf{s}_t, \mathbf{c}_1, \dots, \mathbf{c}_n) \propto P(\mathbf{x}_{t+1} | \mathbf{s}_t) \prod_{i=1}^n \frac{P(\mathbf{x}_{t+1} | \mathbf{s}_t, \mathbf{c}_i)}{P(\mathbf{x}_{t+1} | \mathbf{s}_t)} \quad (11)$$

i.e. only a single token is considered at each generation step, making our formulation compatible with autoregressive (next-token) prediction. In practice, we speculate that the autoregressive case is less compatible with our compositional method than parallel token prediction due to being less strongly regularised (and hence more prone to over-fitting: parallel token prediction is strongly regularised by design [9]), in addition to being more sensitive to the accumulation of errors due to tokens being generated “left-to-right, top to bottom” in the image. Furthermore, there is no guarantee that autoregressive models provide a calibrated estimate of conditional/unconditional probabilities, which may further limit hypothetical performance. For these reasons, we maintain our focus on parallel token prediction which is found to outperform the previous state-of-the-art on image generation accuracy when applied alongside our discrete composition method.

## F Additional Qualitative Experiments

### F.1 Conceptual Product Space

Fig. 10 illustrates how our compositional method can be used to generate a “product space” over visual concepts. In particular, Fig. 10 demonstrates the Cartesian product of the “colour” concept {"a red object", "an orange object", ...} with the “category” concept {"a cat", "a dog", "an apple", "a cherry"} using our approach. Concept weights  $w_1$  and  $w_2$  are set at 6 for all samples. We used the aMUSED [15] implementation of MUSE [11] (text-to-image masked generative transformer) as the pre-trained backbone model, as with other qualitative text-to-image experiments.





Figure 10: Conceptual product space: Example of composing two concept spaces using our framework: {"a cat", "a dog", "an apple", "a cherry"}  $\times$  AND {"a red object", "an orange object", "a yellow object", "a green object", "a blue object", "an indigo object", "a violet object"}.

## F.2 Varying Concept Weight for FFHQ

In the main text we visualise the effect of varying  $w_{male}$  for the FFHQ dataset. Figures 11 and 12 visualise the effect of varying the weights of the remaining two concepts in FFHQ ( $w_{no\_glasses}$  and  $w_{smile}$  respectively).

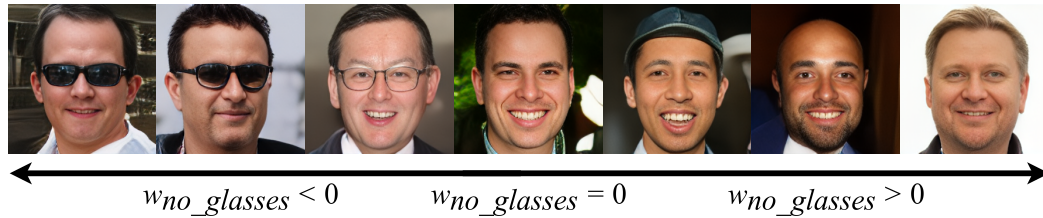


Figure 11: Effect of varying the  $w_{no\_glasses}$  concept weight from  $-3.0$  to  $3.0$  while keeping  $w_{male} = w_{smile} = 3.0$ .

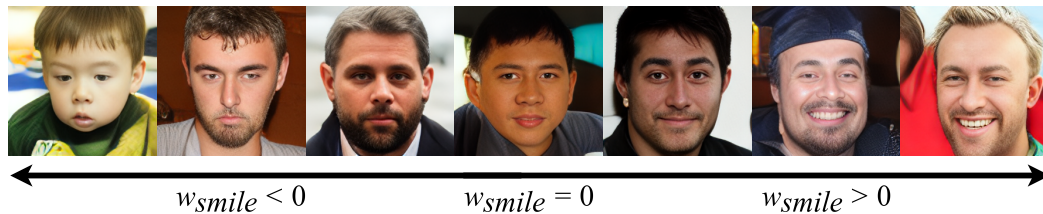


Figure 12: Effect of varying the  $w_{no\_glasses}$  concept weight from  $-3.0$  to  $3.0$  while keeping  $w_{male} = w_{no\_glasses} = 3.0$ .

## G Full Model Training Details

Here we give the full technical details of our training runs in addition to hardware considerations.

For each dataset, we utilise a deep residual convolutional vector-quantized autoencoder architecture following the protocol of [8] and [9] which have been previously shown to produce high-fidelity reconstructions for a variety of image datasets. We use a training batch size of 20 for CLEVR and Relational CLEVR, with a smaller batch size of 8 for FFHQ due to the larger image size. CLEVR and Compositional CLEVR VQ-VAE models are trained for 20,000 iterations each, while the FFHQ VQ-GAN is trained for 100,000 iterations due to the smaller batch size and larger resolution, with adversarial loss starting at 30,000 iterations.

We set the VQ-VAE/VQ-GAN codebook size at 256 for all three datasets, which we find to be sufficient for obtaining high-quality reconstructions. We use the encoder-only transformer architecture, using the exact same architecture for all three datasets (from [9]) (24 layer, embedding dimension 512, fully connected hidden dimension 2048). We train a total of 3 samplers (one for each dataset) for 300,000 iterations each. Training each sampler model took 1.5 days per model, with an additional 0.5 days for evaluations. Training of all models and running evaluation took approximately 5 days in total, using a single NVIDIA GeForce RTX 3090 and Pytorch implementations (see code in supplementary). Preliminary and failed experiments (e.g. due to bugs) made up for around 3 days of compute on the same hardware.

For each dataset, we encode input conditions as additional embeddings which are concatenated to the latent embeddings before being fed to the transformer. Object position for CLEVR is encoded using a learned linear map  $M_{pos} : \mathbb{R}^2 \rightarrow \mathbb{R}^d$  where  $d$  is the hidden dimension of the transformer. Face attributes for FFHQ are encoded using learned embedding  $M_{face} : \{\text{“smile”, “no smile”, “glasses”, “no glasses”, “female”, “male”}\} \rightarrow \mathbb{R}^d$ . For Relational CLEVR, we tokenize text descriptions, mapping to learned token embeddings and adding positional embeddings before concatenating with the learned image token embeddings (also adding learned position embeddings for the image token embeddings).

## H Baselines Details

In the quantitative evaluations of our method, we compare against the baseline results provided in [7] in addition to the results of the method in [7]. For completeness, below we provide a brief description of how the baseline results were obtained in [7]:

- **StyleGAN2-ADA** [27] - The StyleGAN2-ADA results were obtained in [7] using the off-the-shelf model provided by [27].
- **StyleGAN2** [28] - Compositional StyleGAN2 results were obtained in [1] by training classifiers on the latent space of StyleGAN2, which were then used to generate novel latent representations. StyleGAN2 models were either used off-the-shelf (for FFHQ) or trained from scratch (for Positional and Relational CLEVR).
- **LACE** [5] - LACE results were obtained in [7] by composing energy-based models acting on the latent space as in [5], with training data generated by StyleGAN2-ADA (above).
- **GLIDE** [29] - The (non-composed) GLIDE results were obtained in [7] by encoding input conditions as a single, long sentence, with outputs being upsampled separately from  $64 \times 64$ .
- **EBM** [6] - Composed EBM results were obtained in [7] by composing conditional energy functions for multiple concepts as in [6].
- **Composed GLIDE** [7] - Composed GLIDE results were obtained by [7] using the method for composing diffusion outputs proposed by [7].

We had insufficient resources to train our own models from scratch, and so we instead precisely replicated the evaluation protocol of [7] to enable fair comparison with our own method.

## I Binary Classifier Details

In the main text we include generation accuracy metrics for baseline methods (from [7]) and our own experiments with Positional CLEVR, Relational CLEVR and FFHQ. Here we document fully how we obtained our own accuracy scores by following the evaluation approach of [7] so as to maintain valid comparisons with the baseline results reported by [7].

Accuracy is determined by a binary classifier for each of the three datasets, which takes both an image and an attribute as input and produces a binary output corresponding to whether the specified attribute is present. We obtained the accuracy scores following the exact same evaluation approach of [7] so as to maintain valid comparisons with the baseline results reported by [7]. For each experiment we generate 5000 images, computing accuracy (Acc) and FID for each group of 5000. Samples are taken over 30 time steps (corresponding to unmasking  $256/30 \approx 8.53$  tokens per time step on average). We fix the concept weight  $w_i$  at 3.0 for all experiments. We detail all quantitative results in Table 1 and in Tables 3 and 4 in Appendix C (best performance is written in bold for each column, second-best is underlined).

For CLEVR and Relational CLEVR, we use the pre-trained classifiers provided by [7], which have validation classification accuracy scores of 99.05% and 99.80% respectively. For FFHQ, since no pre-trained classifier was available we trained binary classifiers following the same procedure as [7] (one for each attribute, with a 80 : 20 train-validation split). The classifiers achieve equal or greater validation accuracy than the classifiers used by [7]. The high validation accuracy scores for the evaluation classifiers are deemed sufficient to allow reliable estimation of the accuracy for our generated images. Our quantitative evaluations follow the exact same procedure used to obtain the baseline results [7], allowing for fair comparison with the baselines.

## J Standard Uncertainty Computation

In Tables 1, 3 and 4 we include standard uncertainties at two standard deviations ( $2\sigma$ ). We base this computation on the number of sampled images in order to give context to the difference between baseline results and our own results (this is especially useful when results are close together). We are unable to report error bars based on multiple repeats of training runs because such error bars were not reported in [7] and we lack the resources to perform our own runs of their experiments. For these reasons, the value of  $2\sigma$  (two standard deviations) is derived and computed as follows for a percentage accuracy score  $p$ :

We assume that a given method generates an image correctly (consistent with the specified conditions) with probability  $p$ , independently for each of  $n$  trials (generated samples). It follows that the number of "correct" samples  $X$  is distributed according to the Binomial distribution:

$$X \sim B(n, p) \tag{12}$$

The variance in the number of correct samples  $X$  is then:

$$Var(X) = np(1 - p) \tag{13}$$

And thus the standard deviation is:

$$SD(X) = \sqrt{np(1 - p)} \tag{14}$$

The standard deviation  $\sigma$  of the accuracy score is then  $SD(X)$  divided by  $n$ :

$$\sigma = \frac{\sqrt{np(1 - p)}}{n} \tag{15}$$

$$= \frac{\sqrt{p(1 - p)}}{\sqrt{n}} \tag{16}$$

$$= \sqrt{\frac{p(1 - p)}{n}} (\times 100\%) \tag{17}$$

$$\tag{18}$$

Finally, we clip values for  $2\sigma$  to be no greater than  $p$  and no greater than  $1 - p$  so as to avoid giving error bounds greater than 100% or smaller than 0%. We compute  $2\sigma$  in the same way for all accuracy results (including those reported by [7]) since they are all computed based on 5000 generated samples.



Figure 13: Perceptual nearest neighbours for the (positional) CLEVR dataset. Leftmost column is (non-cherry-picked) generated samples, remaining images in each row are the 8 nearest neighbours (left to right goes from nearest to farthest).

We omit uncertainties for FID for two reasons: (1) the uncertainty in FID for comparing two sets of 5000 images is expected to be low [26] and (2) it would take too long with our available computational resources to compute these by repeating all experiments (including running the baselines) multiple times.

## K Nearest Neighbours of Generated Samples

To verify that our method does not simply reproduce samples from the training data (over-fitting), for each dataset we generate a batch of 8 images based on a random selection of 3 input conditions (positions, relations and attributes for CLEVR, Relational CLEVR and FFHQ respectively). In this experiment, we choose to study the composition of 3 input conditions (as opposed to 1 or 2) as this situation is the most likely to produce over-fit images (due to it finding the "smallest", or lowest-entropy section of the sample space). We compute the 8 nearest neighbours of each sample from the original training data based on perceptual distance. Figures 13, 14 and 15 visualise the results. The leftmost column of each figure contains the (non-cherry-picked) generated samples, while the remaining 8 images in each row are the nearest neighbours. These figures show qualitatively that none of the 8 generated samples from each dataset perfectly match the nearest neighbours, indicating strong generalisation performance. All samples were taken at temperature 0.9 and condition weight 3.0, in accordance with quantitative experiments in the main text.

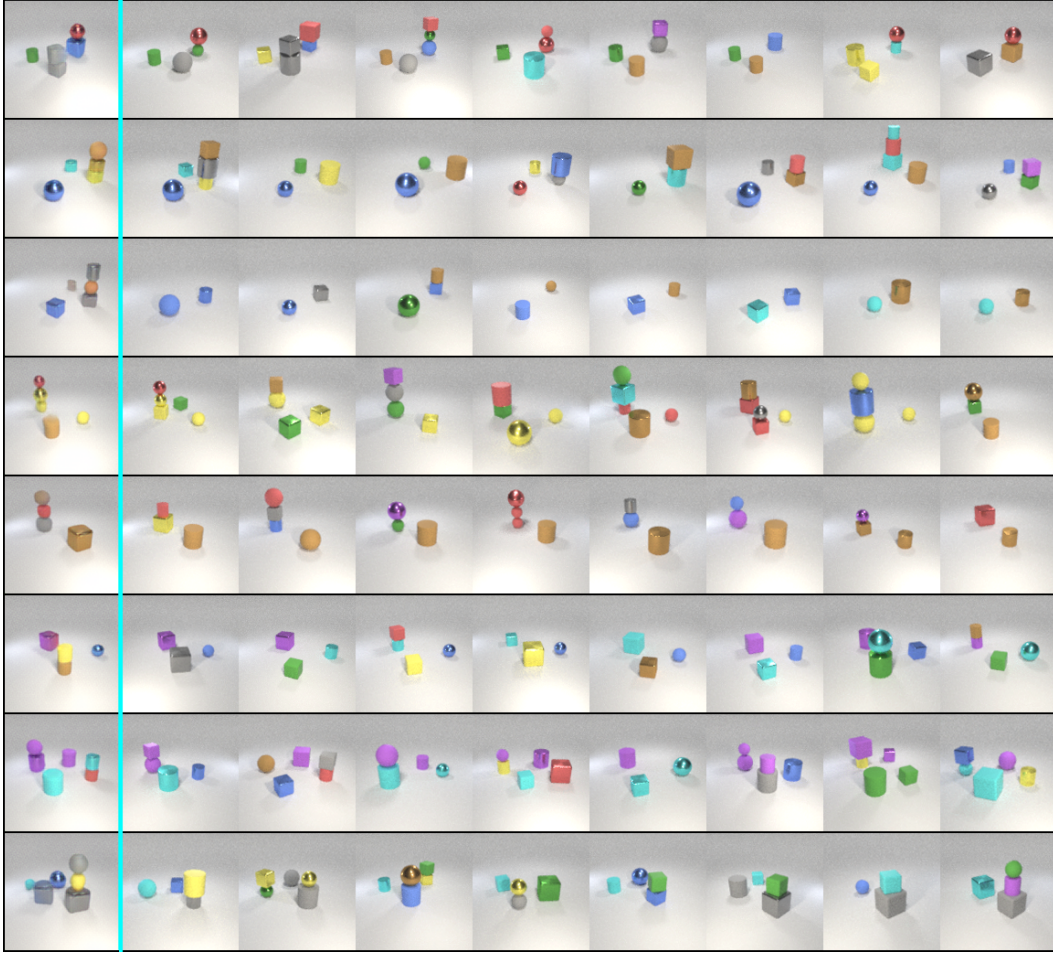


Figure 14: Perceptual nearest neighbours for the Relational CLEVR dataset. Leftmost column is (non-cherry-picked) generated samples, remaining images in each row are the 8 nearest neighbours (left to right goes from nearest to farthest).

## L Code License and Running Instructions

Please see LICENSE in the code for full license(s).

Please see README.md in the code for running instructions for reproducing our quantitative experiments, including model training, classifier training, and obtaining results.



Figure 15: Perceptual nearest neighbours for the FFHQ dataset. Leftmost column is (non-cherry-picked) generated samples, remaining images in each row are the 8 nearest neighbours (left to right goes from nearest to farthest).

## NeurIPS Paper Checklist

### 1. Claims

Question: Do the main claims made in the abstract and introduction accurately reflect the paper’s contributions and scope?

Answer: [\[Yes\]](#)

Justification: The paper includes our mathematical formulation, quantitative experimental results, and qualitative visual examples that reflect and justify the claims in our abstract and introduction.

Guidelines:

- The answer NA means that the abstract and introduction do not include the claims made in the paper.
- The abstract and/or introduction should clearly state the claims made, including the contributions made in the paper and important assumptions and limitations. A No or NA answer to this question will not be perceived well by the reviewers.
- The claims made should match theoretical and experimental results, and reflect how much the results can be expected to generalise to other settings.
- It is fine to include aspirational goals as motivation as long as it is clear that these goals are not attained by the paper.

## 2. Limitations

Question: Does the paper discuss the limitations of the work performed by the authors?

Answer: [Yes]

Justification: The discussion section contains a discussion of our method's limitations.

Guidelines:

- The answer NA means that the paper has no limitation while the answer No means that the paper has limitations, but those are not discussed in the paper.
- The authors are encouraged to create a separate "Limitations" section in their paper.
- The paper should point out any strong assumptions and how robust the results are to violations of these assumptions (e.g., independence assumptions, noiseless settings, model well-specification, asymptotic approximations only holding locally). The authors should reflect on how these assumptions might be violated in practice and what the implications would be.
- The authors should reflect on the scope of the claims made, e.g., if the approach was only tested on a few datasets or with a few runs. In general, empirical results often depend on implicit assumptions, which should be articulated.
- The authors should reflect on the factors that influence the performance of the approach. For example, a facial recognition algorithm may perform poorly when image resolution is low or images are taken in low lighting. Or a speech-to-text system might not be used reliably to provide closed captions for online lectures because it fails to handle technical jargon.
- The authors should discuss the computational efficiency of the proposed algorithms and how they scale with dataset size.
- If applicable, the authors should discuss possible limitations of their approach to address problems of privacy and fairness.
- While the authors might fear that complete honesty about limitations might be used by reviewers as grounds for rejection, a worse outcome might be that reviewers discover limitations that aren't acknowledged in the paper. The authors should use their best judgment and recognize that individual actions in favor of transparency play an important role in developing norms that preserve the integrity of the community. Reviewers will be specifically instructed to not penalise honesty concerning limitations.

## 3. Theory Assumptions and Proofs

Question: For each theoretical result, does the paper provide the full set of assumptions and a complete (and correct) proof?

Answer: [Yes]

Justification: We state at the beginning of our derivation the only assumption of our method (that conditions are independent), followed by the full derivation of our formulation, with extra intermediate steps in the Appendix.

Guidelines:

- The answer NA means that the paper does not include theoretical results.
- All the theorems, formulas, and proofs in the paper should be numbered and cross-referenced.
- All assumptions should be clearly stated or referenced in the statement of any theorems.
- The proofs can either appear in the main paper or the supplemental material, but if they appear in the supplemental material, the authors are encouraged to provide a short proof sketch to provide intuition.
- Inversely, any informal proof provided in the core of the paper should be complemented by formal proofs provided in appendix or supplemental material.
- Theorems and Lemmas that the proof relies upon should be properly referenced.

## 4. Experimental Result Reproducibility

Question: Does the paper fully disclose all the information needed to reproduce the main experimental results of the paper to the extent that it affects the main claims and/or conclusions of the paper (regardless of whether the code and data are provided or not)?

Answer: [Yes]

Justification: We show how our formulation result can be applied to any discrete generative prior (in addition to specific adaptations to the particular non-autoregressive prior we used). We provide anonymized code for our quantitative experiments alongside clear instructions (README.md) for training and evaluation.

Guidelines:

- The answer NA means that the paper does not include experiments.
- If the paper includes experiments, a No answer to this question will not be perceived well by the reviewers: Making the paper reproducible is important, regardless of whether the code and data are provided or not.
- If the contribution is a dataset and/or model, the authors should describe the steps taken to make their results reproducible or verifiable.
- Depending on the contribution, reproducibility can be accomplished in various ways. For example, if the contribution is a novel architecture, describing the architecture fully might suffice, or if the contribution is a specific model and empirical evaluation, it may be necessary to either make it possible for others to replicate the model with the same dataset, or provide access to the model. In general, releasing code and data is often one good way to accomplish this, but reproducibility can also be provided via detailed instructions for how to replicate the results, access to a hosted model (e.g., in the case of a large language model), releasing of a model checkpoint, or other means that are appropriate to the research performed.
- While NeurIPS does not require releasing code, the conference does require all submissions to provide some reasonable avenue for reproducibility, which may depend on the nature of the contribution. For example
  - (a) If the contribution is primarily a new algorithm, the paper should make it clear how to reproduce that algorithm.
  - (b) If the contribution is primarily a new model architecture, the paper should describe the architecture clearly and fully.
  - (c) If the contribution is a new model (e.g., a large language model), then there should either be a way to access this model for reproducing the results or a way to reproduce the model (e.g., with an open-source dataset or instructions for how to construct the dataset).
  - (d) We recognize that reproducibility may be tricky in some cases, in which case authors are welcome to describe the particular way they provide for reproducibility. In the case of closed-source models, it may be that access to the model is limited in some way (e.g., to registered users), but it should be possible for other researchers to have some path to reproducing or verifying the results.

## 5. Open access to data and code

Question: Does the paper provide open access to the data and code, with sufficient instructions to faithfully reproduce the main experimental results, as described in supplemental material?

Answer: [Yes]

Justification: We provide anonymized code for our quantitative experiments alongside clear instructions (README.md) for training and evaluation.

Guidelines:

- The answer NA means that paper does not include experiments requiring code.
- Please see the NeurIPS code and data submission guidelines (<https://nips.cc/public/guides/CodeSubmissionPolicy>) for more details.
- While we encourage the release of code and data, we understand that this might not be possible, so “No” is an acceptable answer. Papers cannot be rejected simply for not including code, unless this is central to the contribution (e.g., for a new open-source benchmark).
- The instructions should contain the exact command and environment needed to run to reproduce the results. See the NeurIPS code and data submission guidelines (<https://nips.cc/public/guides/CodeSubmissionPolicy>) for more details.



- The authors should provide instructions on data access and preparation, including how to access the raw data, preprocessed data, intermediate data, and generated data, etc.
- The authors should provide scripts to reproduce all experimental results for the new proposed method and baselines. If only a subset of experiments are reproducible, they should state which ones are omitted from the script and why.
- At submission time, to preserve anonymity, the authors should release anonymized versions (if applicable).
- Providing as much information as possible in supplemental material (appended to the paper) is recommended, but including URLs to data and code is permitted.

## 6. Experimental Setting/Details

Question: Does the paper specify all the training and test details (e.g., data splits, hyper-parameters, how they were chosen, type of optimizer, etc.) necessary to understand the results?

Answer: [Yes]

Justification: Full training and testing details are in appendix. Full implementations of generative models and classifiers are included in code.

Guidelines:

- The answer NA means that the paper does not include experiments.
- The experimental setting should be presented in the core of the paper to a level of detail that is necessary to appreciate the results and make sense of them.
- The full details can be provided either with the code, in appendix, or as supplemental material.

## 7. Experiment Statistical Significance

Question: Does the paper report error bars suitably and correctly defined or other appropriate information about the statistical significance of the experiments?

Answer: [Yes]

Justification: For results on generation accuracy (Acc.), we include error bars at  $\pm 2\sigma$  derived from the number of trials (5000). For FID results we explain why this is not possible

Guidelines:

- The answer NA means that the paper does not include experiments.
- The authors should answer "Yes" if the results are accompanied by error bars, confidence intervals, or statistical significance tests, at least for the experiments that support the main claims of the paper.
- The factors of variability that the error bars are capturing should be clearly stated (for example, train/test split, initialization, random drawing of some parameter, or overall run with given experimental conditions).
- The method for calculating the error bars should be explained (closed form formula, call to a library function, bootstrap, etc.)
- The assumptions made should be given (e.g., Normally distributed errors).
- It should be clear whether the error bar is the standard deviation or the standard error of the mean.
- It is OK to report 1-sigma error bars, but one should state it. The authors should preferably report a 2-sigma error bar than state that they have a 96% CI, if the hypothesis of Normality of errors is not verified.
- For asymmetric distributions, the authors should be careful not to show in tables or figures symmetric error bars that would yield results that are out of range (e.g. negative error rates).
- If error bars are reported in tables or plots, The authors should explain in the text how they were calculated and reference the corresponding figures or tables in the text.

## 8. Experiments Compute Resources

Question: For each experiment, does the paper provide sufficient information on the computer resources (type of compute workers, memory, time of execution) needed to reproduce the experiments?

Answer: [Yes]

Justification: We include the name of the GPU we used in addition to the time of execution for individual experiments and all experiments in total (in days).

Guidelines:

- The answer NA means that the paper does not include experiments.
- The paper should indicate the type of compute workers CPU or GPU, internal cluster, or cloud provider, including relevant memory and storage.
- The paper should provide the amount of compute required for each of the individual experimental runs as well as estimate the total compute.
- The paper should disclose whether the full research project required more compute than the experiments reported in the paper (e.g., preliminary or failed experiments that didn't make it into the paper).

## 9. Code Of Ethics

Question: Does the research conducted in the paper conform, in every respect, with the NeurIPS Code of Ethics [https://neurips.cc/public/EthicsGuidelines?](https://neurips.cc/public/EthicsGuidelines)

Answer: [Yes]

Justification: We do not work with human participants, and all relevant datasets (FFHQ) have been checked for privacy compliance prior to experiments and submission. We do not release any model that could be considered high-risk, and we offer a discussion of broader societal impacts (including bias and misuse) in our discussion section.

Guidelines:

- The answer NA means that the authors have not reviewed the NeurIPS Code of Ethics.
- If the authors answer No, they should explain the special circumstances that require a deviation from the Code of Ethics.
- The authors should make sure to preserve anonymity (e.g., if there is a special consideration due to laws or regulations in their jurisdiction).

## 10. Broader Impacts

Question: Does the paper discuss both potential positive societal impacts and negative societal impacts of the work performed?

Answer: [Yes]

Justification: Our discussion section has a subsection dedicated to potential societal impacts, including both positive and negative.

Guidelines:

- The answer NA means that there is no societal impact of the work performed.
- If the authors answer NA or No, they should explain why their work has no societal impact or why the paper does not address societal impact.
- Examples of negative societal impacts include potential malicious or unintended uses (e.g., disinformation, generating fake profiles, surveillance), fairness considerations (e.g., deployment of technologies that could make decisions that unfairly impact specific groups), privacy considerations, and security considerations.
- The conference expects that many papers will be foundational research and not tied to particular applications, let alone deployments. However, if there is a direct path to any negative applications, the authors should point it out. For example, it is legitimate to point out that an improvement in the quality of generative models could be used to generate deepfakes for disinformation. On the other hand, it is not needed to point out that a generic algorithm for optimizing neural networks could enable people to train models that generate Deepfakes faster.
- The authors should consider possible harms that could arise when the technology is being used as intended and functioning correctly, harms that could arise when the technology is being used as intended but gives incorrect results, and harms following from (intentional or unintentional) misuse of the technology.

- If there are negative societal impacts, the authors could also discuss possible mitigation strategies (e.g., gated release of models, providing defenses in addition to attacks, mechanisms for monitoring misuse, mechanisms to monitor how a system learns from feedback over time, improving the efficiency and accessibility of ML).

#### 11. Safeguards

Question: Does the paper describe safeguards that have been put in place for responsible release of data or models that have a high risk for misuse (e.g., pretrained language models, image generators, or scraped datasets)?

Answer: [NA]

Justification: Our contribution does not include new datasets or pre-trained models that pose a risk of misuse.

Guidelines:

- The answer NA means that the paper poses no such risks.
- Released models that have a high risk for misuse or dual-use should be released with necessary safeguards to allow for controlled use of the model, for example by requiring that users adhere to usage guidelines or restrictions to access the model or implementing safety filters.
- Datasets that have been scraped from the Internet could pose safety risks. The authors should describe how they avoided releasing unsafe images.
- We recognize that providing effective safeguards is challenging, and many papers do not require this, but we encourage authors to take this into account and make a best faith effort.

#### 12. Licenses for existing assets

Question: Are the creators or original owners of assets (e.g., code, data, models), used in the paper, properly credited and are the license and terms of use explicitly mentioned and properly respected?

Answer: [Yes]

Justification: Code that we derive from earlier work is properly licensed and referenced (see code LICENSE).

Guidelines:

- The answer NA means that the paper does not use existing assets.
- The authors should cite the original paper that produced the code package or dataset.
- The authors should state which version of the asset is used and, if possible, include a URL.
- The name of the license (e.g., CC-BY 4.0) should be included for each asset.
- For scraped data from a particular source (e.g., website), the copyright and terms of service of that source should be provided.
- If assets are released, the license, copyright information, and terms of use in the package should be provided. For popular datasets, [paperswithcode.com/datasets](https://paperswithcode.com/datasets) has curated licenses for some datasets. Their licensing guide can help determine the license of a dataset.
- For existing datasets that are re-packaged, both the original license and the license of the derived asset (if it has changed) should be provided.
- If this information is not available online, the authors are encouraged to reach out to the asset's creators.

#### 13. New Assets

Question: Are new assets introduced in the paper well documented and is the documentation provided alongside the assets?

Answer: [Yes]

Justification: We provide anonymized code for our quantitative experiments alongside clear instructions for training and evaluation.

Guidelines:

- The answer NA means that the paper does not release new assets.
- Researchers should communicate the details of the dataset/code/model as part of their submissions via structured templates. This includes details about training, license, limitations, etc.
- The paper should discuss whether and how consent was obtained from people whose asset is used.
- At submission time, remember to anonymize your assets (if applicable). You can either create an anonymized URL or include an anonymized zip file.

#### 14. Crowdsourcing and Research with Human Subjects

Question: For crowdsourcing experiments and research with human subjects, does the paper include the full text of instructions given to participants and screenshots, if applicable, as well as details about compensation (if any)?

Answer: [NA]

Justification: No human subjects or crowdsourcing were involved in this research.

Guidelines:

- The answer NA means that the paper does not involve crowdsourcing nor research with human subjects.
- Including this information in the supplemental material is fine, but if the main contribution of the paper involves human subjects, then as much detail as possible should be included in the main paper.
- According to the NeurIPS Code of Ethics, workers involved in data collection, curation, or other labor should be paid at least the minimum wage in the country of the data collector.

#### 15. Institutional Review Board (IRB) Approvals or Equivalent for Research with Human Subjects

Question: Does the paper describe potential risks incurred by study participants, whether such risks were disclosed to the subjects, and whether Institutional Review Board (IRB) approvals (or an equivalent approval/review based on the requirements of your country or institution) were obtained?

Answer: [NA]

Justification: No human subjects were involved in this research.

Guidelines:

- The answer NA means that the paper does not involve crowdsourcing nor research with human subjects.
- Depending on the country in which research is conducted, IRB approval (or equivalent) may be required for any human subjects research. If you obtained IRB approval, you should clearly state this in the paper.
- We recognize that the procedures for this may vary significantly between institutions and locations, and we expect authors to adhere to the NeurIPS Code of Ethics and the guidelines for their institution.
- For initial submissions, do not include any information that would break anonymity (if applicable), such as the institution conducting the review.